

# A high-resolution mill pond record from eastern Virginia (USA) reveals the impact of past landscape changes and regional pollution history



Nicholas L. Balascio<sup>a,\*</sup>, James M. Kaste<sup>a</sup>, Meredith G. Meyer<sup>a</sup>, Madison Renshaw<sup>a</sup>,  
Kassandra Smith<sup>a</sup>, Randolph M. Chambers<sup>b</sup>

<sup>a</sup> Department of Geology, College of William & Mary, Williamsburg, VA 23187, United States

<sup>b</sup> Keck Environmental Laboratory, College of William & Mary, Williamsburg, VA 23187, United States

## ARTICLE INFO

### Article history:

Received 30 October 2018

Received in revised form 12 January 2019

Accepted 14 January 2019

Available online 15 January 2019

### Keywords:

Mill pond

Legacy sediment

Lead pollution

Atlantic Coastal Plain

Williamsburg

Virginia

## ABSTRACT

Mill ponds appeared throughout the eastern United States following European settlement. Sedimentation in these systems records centuries of past landscape change. To date, mill ponds on the Atlantic Coastal Plain have received little attention, yet this region had the earliest colonial settlements. Mill ponds here also have potential to record geomorphic change and pollution histories at high-resolution because of easily erodible underlying unconsolidated sediments. This paper presents a c. 300-year record of sedimentation in Lake Matoaka, a former mill pond in Williamsburg, Virginia. We used lead (Pb) and cesium (Cs) isotopes ( $^{210}\text{Pb}$ ,  $^{137}\text{Cs}$ ), Pb concentrations, stable Pb isotopes ( $^{206}\text{Pb}/^{207}\text{Pb}$ ), and chronostratigraphic horizons to develop a chronology, which shows remarkably high sedimentation rates,  $\sim 0.5$  cm/yr. Sedimentological data including the analysis of organic matter, grain size, and elemental compositions, revealed past conditions within the lake and its watershed. These data are linked to the operation of the mill c. CE 1700–1910, changes in the dam structure, and other historic developments of the region. Tracing pollution history with  $^{206}\text{Pb}/^{207}\text{Pb}$  showed mid-1800s atmospheric deposition from smelting of Upper Mississippi Valley district Pb ores, and a sharp maxima in total Pb of 134  $\mu\text{g/g}$  in the 1970s from the peak use of leaded gasoline in North America. Mass accumulation rates climbed from c. 0.08 to 0.28 g/cm/yr during the 18th and 19th centuries from deforestation and agriculture, which is somewhat lower than sediment yields documented in other regions. We suggest that stream channel storage may buffer pond sedimentation within low gradient, coastal plain landscapes. This study contributes to the understanding of sedimentation in mill ponds for reconstructing historic landscape changes and regional pollution history.

© 2019 Elsevier Ltd. All rights reserved.

## 1. Introduction

Extensive damming of streams to provide waterpower for mills and other agricultural and industrial processes began following European settlement of the eastern United States (U.S.) in the 1600s (Walter and Merritts, 2008). The states of Pennsylvania, Maryland, and Virginia each had tens of thousands of mill dams during the 17<sup>th</sup>–19<sup>th</sup> centuries (Walter and Merritts, 2008; Pizzuto and O'Neal, 2009). Dams and their subsequent abandonment significantly impacted fluvial geomorphologic processes at local and regional scales (Price and Leigh, 2006; Walter and Merritts, 2008; Pizzuto and O'Neal, 2009; Kennedy, 2016). Furthermore, sediments accumulated behind these dams from forest clearing and agriculture starting in colonial times (“legacy sediments”;

James, 2013) are a modern source of nutrients and pollution that can be remobilized and degrade downstream ecosystems (Niemitz et al., 2013; Coxon et al., 2016). In most places, these dams formed mill ponds, many of which were maintained following the termination of mill operations. Some mill ponds contain continuous sediment records of landscape change and pollution history (Arnason and Fletcher, 2003; Van Metre and Mahler, 2004; Mann et al., 2013; Fajer and Rzetala, 2018), similar to those developed from natural lakes (e.g. Davis et al., 2006; Liu et al., 2012). Analysis of mill pond sediments can therefore: (i) inform our understanding about the characteristics of legacy sediments in different environments, (ii) provide highly resolved records of landscape change that can augment historic records and document the response of lakes and their catchments to past human activities, and (iii) provide an inventory of local and regional pollutants.

Previous studies of mill pond records and legacy sediments have focused on bedrock dominated physiographic regions of the eastern U.S. (e.g., Walter and Merritts, 2008; Pizzuto and O'Neal,

\* Corresponding author.

E-mail address: [nbalascio@wm.edu](mailto:nbalascio@wm.edu) (N.L. Balascio).

2009). Extensive damming also occurred in streams of the Atlantic Coastal Plain, however, and sediment dynamics here are unique given that the landscape is composed of unconsolidated fluvial and shallow marine deposits (Markewich et al., 1990). High-density drainage networks in the Coastal Plain carry significant sediment loads even during moderate precipitation events, and suspended sediment concentrations exceed 1 g/l during intense thunderstorms and low-pressure systems (Lecce et al., 2006; Caverly et al., 2013).

Here we provide a detailed analysis of sediments accumulated since c. CE 1700 in Lake Matoaka, a former mill pond in Williamsburg, Virginia, USA (Fig. 1). We evaluate how changes in the function of the lake, early landscape activity, historic events, and 20<sup>th</sup> century regional industrial activity impacted the watershed and sedimentation in this coastal plain lake. We develop a robust chronology using multiple dating techniques, including lead (Pb) and cesium (Cs) isotopes ( $^{210}\text{Pb}$ ,  $^{137}\text{Cs}$ ), Pb concentrations, and stable Pb isotopes ( $^{206}\text{Pb}/^{207}\text{Pb}$ ), and present detailed sedimentological data to interpret past conditions within the lake and watershed. Overall, this reconstruction documents the

evolution of the basin from an early colonial-era mill pond to an artificial lake, helping us describe the evolution of coastal plain landscapes in response to anthropogenic impacts. This study also demonstrates how coastal plain lakes and mill ponds can archive regional pollution history at high-resolution.

## 2. Study site and watershed history

Lake Matoaka ( $37^{\circ}15.878'\text{N}$   $76^{\circ}43.386'\text{W}$ ; 7 m asl) is located in southeastern Virginia on the College of William & Mary campus in Williamsburg (Fig. 1 and 2). Several narrow valleys confine the lake, which has an area of 0.17 km<sup>2</sup>, a maximum depth of 4.8 m, and a 6 km<sup>2</sup> catchment within the Atlantic Coastal Plain Province. Today, the catchment is ~60% forested with the remaining ~40% a mix of commercial and residential land uses, as well as buildings associated with the college. The largest stream is College Creek, which flows from north to south into the main arm of the lake, but there are several smaller tributary streams that drain the catchment (Fig. 1). The catchment is composed of Pliocene shallow marine and intertidal deposits of the Bacons Castle and Yorktown

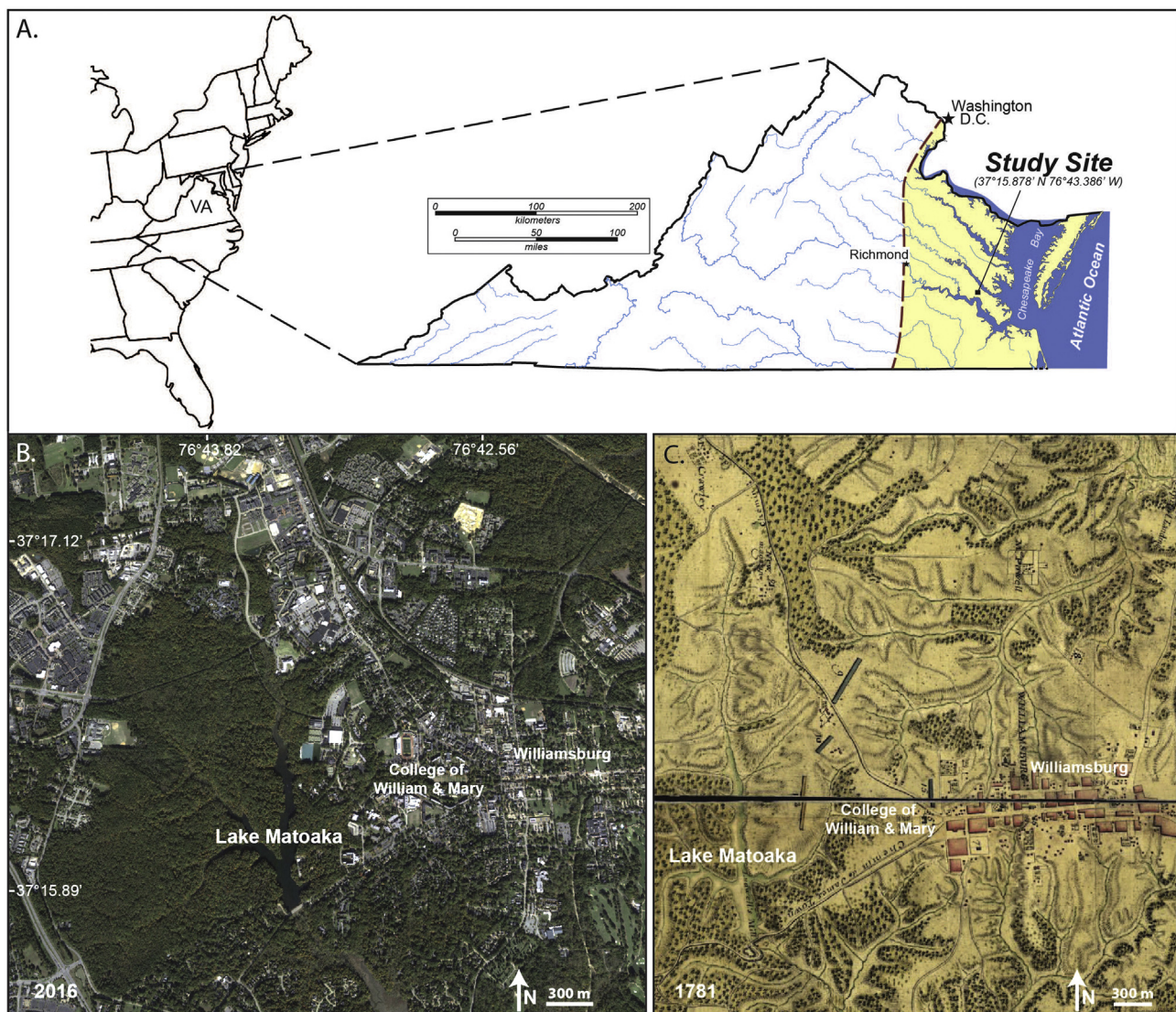


**Fig. 1.** (A.) Location of Virginia in the mid-Atlantic region of the United States, and Williamsburg in the Coastal Plain Province (yellow shaded region) of eastern Virginia. (B.) Aerial photograph of Lake Matoaka and its catchment indicating the location of Williamsburg and the College of William & Mary campus (Map data: Google, 2016). (C.) Historical map of Williamsburg from CE 1781 during the Revolutionary War that shows Williamsburg and the majority of the Lake Matoaka (Ludwell's Mill) catchment (Scale: c. 1:15,250; Desandrouins, 1782) (For interpretation of the references to colour in this figure legend, the reader is referred to the web version of this article).



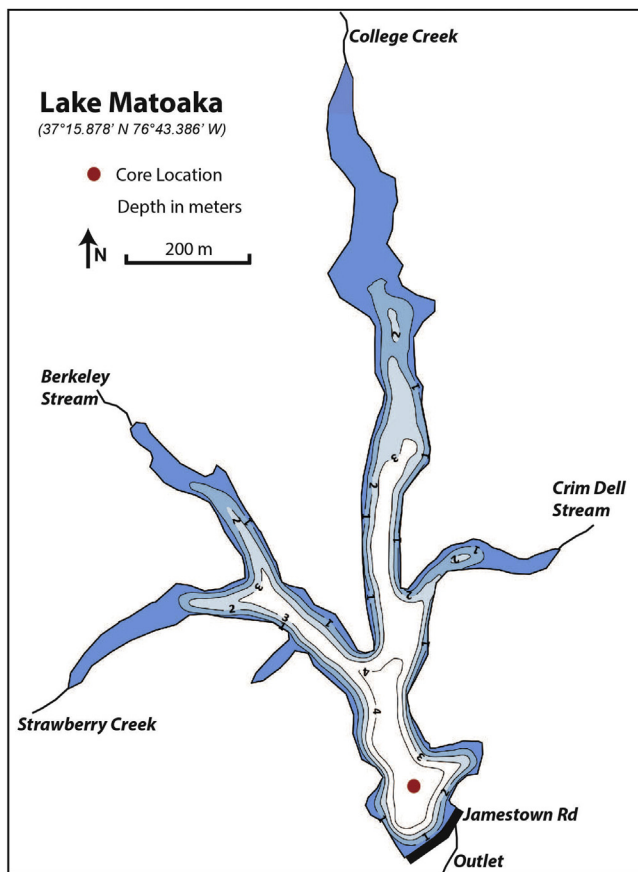


**Fig. 2.** Bathymetric map of Lake Matoaka showing the location of core LMP-03-16, the dam along Jamestown Road, and the major tributary streams.

Formations, with the Yorktown Formation located in the valley bottoms and containing sandy and shell-rich sediments (Mixon et al., 1989).

Lake Matoaka is a former mill pond, impounded by a dam at its southern end along Jamestown Road (Figs. 1 and 2). Before emplacement of the dam, the drainage was known as Archer's Hope Swamp and the main creek flowing through the valley as Archer's Hope Creek, which today is named College Creek. Historic transactional property records indicate that the lake was formed c. CE 1700 when a dam was constructed to power a gristmill known as Ludwell's Mill and later Jones' Mill (Will of William Broadribb, 1905; Stephenson, 1947; Chappell, 1971), making this dam perhaps the oldest artificial pond still maintained on the Coastal Plain. Construction of the College of William & Mary began around the same time, CE 1695, but the college buildings had limited extent and the catchment was primarily a mix of forested and agricultural land until the 20<sup>th</sup> century. In 1925, the College of William & Mary acquired the lake and a majority of the land within its catchment. The lake was renamed Lake Matoaka (Note: Historical documents before CE 1925 referred to this lake as Ludwell's Mill Pond and later Jones' Pond; however, this paper refers to it as Lake Matoaka throughout for consistency). Because of the proximity of Lake Matoaka and its catchment to the town center, changes in sedimentary dynamics can be directly linked to historic development of Williamsburg.

During the 20<sup>th</sup> century, human activities heavily impacted the lake and most significantly, the dam was widened in CE 1907 when the road over the dam was re-graded and paved as part of an early road-building project (Virginia State Highway Commission, 1907). In addition, over the last 100 years, the College of William & Mary

progressively expanded toward the eastern shore of the lake and the population of Williamsburg increased. Development in the catchment has led to changes in sedimentation, excess nutrient loading, and eutrophication of the lake in recent decades and today it is designated hyper-eutrophic (Nielson et al., 1990; Pensa and Chambers, 2004). Analysis of the deltas formed in front of the primary inlet streams has also shown that College Creek and Crim Dell input the most sediment, which are the sub-watersheds that have been most extensively developed (Pensa and Chambers, 2004) (Fig. 1).

### 3. Methods

We evaluated the sedimentation history of Lake Matoaka by analyzing a core recovered from the deepest part of the lake. We performed a variety of physical and geochemical analyses to date the sediments and assess changes in past conditions within and around the lake over the past c. 300 years.

#### 3.1. Sediment core collection and analysis

A depth sounder with integrated GPS recorded bathymetric profiles for creation of a bathymetric map (Fig. 2). A sediment core was collected in 2016 (LMP-03-16; 148 cm) using a push-coring system with piston. The core was recovered with an intact sediment-water interface and penetrated through the lacustrine sediments. The core was split, described, and photographed. A Bartington MS2E sensor measured the magnetic susceptibility of the core every 0.5 cm. The core was then sampled volumetrically at 0.5-cm intervals to measure the dry bulk density, which was calculated as the mass of 1cm<sup>3</sup> samples after freeze drying.

#### 3.2. Organic matter properties

Sedimentary organic matter can be related to environmental factors that affect lake productivity, organic matter preservation, and the delivery of organic matter (Meyers, 2003). We measured total organic carbon (TOC), total nitrogen (TN), biogenic silica (BSi), and sulfur. The TOC can indicate changes in the input of terrestrial-derived organic matter or changes in primary productivity driven by nutrient availability or lake water temperature (Meyers, 2003). The ratio of TOC to TN (C/N) reflects the relative proportion of aquatic- versus terrestrial-derived organic matter, with C/N values from 4 to 10 typical of algae and values greater than 10 attributed to a greater contribution by terrestrial plants (Meyers, 2003). Biogenic silica indicates diatom abundance (Conley, 1988; Conley and Schelske, 2001), which is often used as a proxy for lake productivity (Battarbee et al., 2001). Sulfur in lake sediments can be in organic and inorganic forms related to the sulfate concentrations in the lake water as well as the degree of sulfate reduction (Mitchell et al., 1988), which in the presence of iron can precipitate iron sulfide. Sulfur in most freshwater lakes is generally low, but can be delivered to a lake as sulfate from weathering of minerals in the catchment or atmospheric inputs (Holmer and Storkholm, 2001). The ratio of organic carbon to sedimentary sulfur (C/S) indicates the relative input of organic versus inorganic sulfur where higher values may indicate greater organic sulfur and lower values greater inorganic sulfur.

An Elementar vario MICRO cube elemental analyzer measured the TOC, TN, and sulfur content of select samples. Samples were freeze-dried, ground, and acidified with 10% hydrochloric acid prior to analysis. Uncertainties in weight percent nitrogen, carbon, and sulfur values are within 0.04%, 0.2%, and 0.04%, respectively based on triplicate analysis. The molar ratio of TOC to TN (C/N) was calculated for each sample. Biogenic silica was also measured on the same set of samples following methods similar to Mortlock and

Froelich (1989). Briefly, freeze-dried sediment was ground and 50–80 mg were weighed into centrifuge tubes. Samples were pre-treated with 5 ml of 30% hydrogen peroxide to remove organic material and with 5 ml of 1 M hydrochloric acid to remove carbonate. Biogenic silica was then extracted using 40 ml of 10% sodium carbonate for 5 h in an oven at 80 °C. Biogenic silica concentrations were determined using molybdate-blue reduction and analyzed on an AquaMate Plus UV–vis spectrophotometer for absorbance at 812 nm. Silica standards were used to calibrate absorbance and concentrations were converted to percent biogenic silica.

### 3.3. Grain size analysis

Grain size distributions throughout the record were examined to understand changes in the flux of lithogenic sediment to Lake Matoaka. Grain size data can indicate a variety of catchment processes, including changes in: runoff, land use, sediment supply, and sediment source. Grain size analysis was performed on a total of 68 samples taken from throughout the core. Samples were pretreated with 10 ml of 30% hydrogen peroxide for 48 h to remove organic matter, and for 24 h with 10 ml of hexametaphosphate to disaggregate particles before analysis on a Beckman Coulter LS13320 laser diffraction particle size analyzer.

### 3.4. Scanning X-ray fluorescence

To characterize sedimentary changes at high resolution, an Itrax<sup>TM</sup> X-ray fluorescence (XRF) core scanner at Lamont-Doherty Earth Observatory was used to measure geochemical compositions of the sediment cores every 0.2 cm (Croudace et al., 2006; Rothwell et al., 2006). The Itrax nondestructively scans the surface of split cores and outputs elemental compositions as peak areas from dispersive energy spectrum reflecting their relative concentration in the sediment. Elemental changes are often related to the source and compositions of lithogenic sediments, but some elements can also be linked to biological or redox processes. A molybdenum tube and exposure time of 10 s were used to acquire data for a suite of elements (Table 1). The analysis focused on: silicon (Si), sulfur (S), potassium (K), calcium (Ca), titanium (Ti), chromium (Cr), manganese (Mn), iron (Fe), nickel (Ni), copper (Cu), zinc (Zn), rubidium (Rb), strontium (Sr), zirconium (Zr), and Pb. To avoid effects of the sediment matrix on the XRF signal, such as density and water content, which may affect the results and can be independent of elemental compositional changes, the elemental data were divided by the total counts per spectrum. Statistical evaluation of correlation coefficients and a principal component

analysis (PCA) was conducted on the elemental data to identify common trends and modes of variability.

### 3.5. <sup>210</sup>Pb and <sup>137</sup>Cs analysis

Activities of <sup>210</sup>Pb and <sup>137</sup>Cs allowed determination of sedimentation rates in the upper section of the record. Radioactive Cs is present in soils and sediments primarily from atmospheric nuclear weapons testing fallout (Ritchie and McHenry, 1990) which became significant in c. CE 1952 and peaked in 1963–1964 (Beck and Bennett, 2002). Excess <sup>210</sup>Pb activity beyond that supported by in-situ decay of the radon (Rn) isotope <sup>222</sup>Rn is also a commonly applied chronological tool for sediments <125 years old (Appleby, 2001). Activities of <sup>137</sup>Cs, <sup>210</sup>Pb, and the radium (Ra) isotope <sup>226</sup>Ra were measured by ultra-low background gamma spectrometry every 1–2 cm in the upper 63 cm and on 5 additional samples down to 121 cm. Samples were packed in 2 cm diameter containers that were sealed with paraffin wax to retain <sup>222</sup>Rn and counted on a heavily shielded Canberra Broad Energy (BE5030) intrinsic germanium detectors for a minimum of 48 h each. Detector efficiency for U-series radionuclides was calibrated directly using certified uranium ore (Canadian Certified Reference Materials Project BL-4a). A calibrated solution obtained through Eckert & Ziegler provided the efficiency for <sup>137</sup>Cs. The point-source transmission method corrected the self-attenuation of the low-energy <sup>210</sup>Pb photon for each sample (Cutshall et al., 1983).

### 3.6. Nitric-extractable Pb and <sup>206</sup>Pb/<sup>207</sup>Pb analysis

The use of Pb amounts and isotopic compositions in sedimentary archives is useful in reconstructing pollution history, but is also increasingly applied as a chronostratigraphic tool based on correlation with historic anthropogenic activities that released Pb to the atmosphere (Lima et al., 2005; Kemp et al., 2012; McConnell et al., 2018). Anthropogenic Pb emissions from metal smelting, steel and iron manufacturing, mining, and the combustion of coal and gasoline greatly exceed natural sources (Nriagu, 1979). During these processes, Pb was mobilized into the atmosphere (Sturges and Barrie, 1987) and dispersed globally where it can be found in a variety of sedimentary environments (e.g. Murozumi et al., 1969; Boyle et al., 1986; Bollhöfer and Rosman, 2000, 2001; McConnell et al., 2018). In the U.S., Pb emissions increased during the 19<sup>th</sup> century with increased industrial activity and coal combustion. During the 20<sup>th</sup> century, emissions continued to increase from coal and industrial processes, having a short maximum in the 1940s from increased mining and smelting associated with World War II, but most significantly in the latter half of the century from the

**Table 1**  
Correlation coefficients of elements analyzed by scanning XRF. Significantly correlated values are in bold (>0.70).

	Si	S	K	Ca	Ti	Cr	Mn	Fe	Ni	Cu	Zn	Rb	Sr	Zr	Pb
<b>Si</b>	1														
<b>S</b>	−0.31	1													
<b>K</b>	<b>0.73</b>	−0.24	1												
<b>Ca</b>	0.01	−0.26	−0.18	1											
<b>Ti</b>	<b>0.76</b>	−0.13	<b>0.82</b>	−0.37	1										
<b>Cr</b>	−0.01	0.11	0.34	−0.23	0.20	1									
<b>Mn</b>	−0.36	0.65	−0.16	−0.38	−0.09	0.17	1								
<b>Fe</b>	−0.20	0.36	0.18	−0.52	0.07	0.33	0.46	1							
<b>Ni</b>	−0.12	0.02	−0.20	0.02	−0.03	−0.03	0.03	−0.33	1						
<b>Cu</b>	−0.40	0.35	−0.43	0.05	−0.34	0.09	0.38	−0.18	0.47	1					
<b>Zn</b>	−0.26	0.66	−0.09	−0.34	−0.02	0.20	<b>0.87</b>	0.45	0.03	0.40	1				
<b>Rb</b>	0.34	−0.19	0.57	−0.21	0.59	0.28	−0.15	0.02	0.07	−0.19	−0.17	1			
<b>Sr</b>	0.11	−0.34	0.00	<b>0.85</b>	−0.16	−0.14	−0.42	−0.36	−0.09	−0.14	−0.37	−0.06	1		
<b>Zr</b>	0.61	−0.45	0.18	0.39	0.31	−0.29	−0.61	−0.67	0.14	−0.15	−0.55	0.18	0.40	1	
<b>Pb</b>	−0.23	0.51	−0.03	−0.42	0.09	0.41	0.57	0.45	−0.01	0.21	0.66	−0.01	−0.38	−0.50	1

combustion of leaded gasoline. Emissions increased from 1930 to a peak in the early 1970's, and was followed by a decline after 1975 when its use was limited as a result of legislation implemented under the Clean Air Act (Nriagu, 1990).

Lead isotopes provide additional chronologic information because they can establish the source of historic Pb emissions, which in the U.S. has varied over the past few hundred years (Rosman et al., 1997; Graney et al., 1995; Chillrud et al., 2003; Lima et al., 2005; Kemp et al., 2012). Lead ores have distinct isotopic compositions and do not undergo significant fractionation during industrial processes and therefore maintain a signature of the Pb source (Chow and Earl, 1972; Sturges and Barrie, 1987). In the U.S., from AD 1830–1870, Pb was primarily sourced from the Upper Mississippi Valley (UMV), which has distinctly high  $^{206}\text{Pb}/^{207}\text{Pb}$  values of 1.3–1.5 (Heyl et al., 1959, 1974). Prevailing westerly winds transported these emissions to the eastern U.S. where they have been identified in Rhode Island (Lima et al., 2005), New Jersey (Kemp et al., 2012), Chesapeake Bay (Marcantonio et al., 2002), and Bermuda (Kelly et al., 2009). The peak in the relative contribution of Pb from UMV to the overall U.S. production was c. AD 1857–1858. Following this period, regional  $^{206}\text{Pb}/^{207}\text{Pb}$  values declined in the early 20<sup>th</sup> century, which has been linked with an increase in emissions from leaded gasoline with lower  $^{206}\text{Pb}/^{207}\text{Pb}$  values (<1.2). A subsequent rise in values after the AD 1960s marks the decline in use of leaded gasoline and greater contribution of other sources (Lima et al., 2005).

Lead was extracted from sediment samples using hot nitric acid. This extraction does not completely dissolve primary silicate minerals or layered silicates, but it releases Pb adsorbed to mineral

grains and organic matter, and thus quantitatively recovers anthropogenic Pb and any geogenic Pb released and redistributed to the sediments by chemical weathering (Kaste et al., 2006). Briefly, 0.75 g of sediment was ignited in a muffle furnace for 6 h and the ash was dissolved in 10 ml of hot trace-metal grade concentrated nitric acid for 30 min. Afterwards, the nitric acid was filtered and diluted to 50 ml and analyzed for Pb content using an axial inductively coupled plasma (ICP) optical emission spectrometer. Blanks were run every 12 samples and always below detection limit. A subset of the nitric acid extractions were run for  $^{206}\text{Pb}/^{207}\text{Pb}$  using an ICP-mass spectrometer at the Dartmouth College Trace Element Analysis Core. Precision on  $^{206}\text{Pb}/^{207}\text{Pb}$  determinations was better than 0.1% based on 10 repeated measurements of National Institute of Standards and Technology Standard 981.

## 4. Results and interpretation

### 4.1. Sediment stratigraphy

Core LMP-03-16 consists of two main lithostratigraphic units (Fig. 3). The lower 22 cm is a dense (average  $0.79\text{ g cm}^{-3}$ ), sandy, organic-rich peat. At 126 cm, there is an abrupt transition to less dense ( $0.11\text{--}0.57\text{ g cm}^{-3}$ ) light brown, clayey silt composition with some coarse intervals, and with terrestrial macrofossil fragments visible throughout. Three sections in the lower part of the core (126–112 cm, 114 cm–90 cm, 72–60 cm) contain coarse sandy layers and abundant terrestrial plant macrofossils. We interpret the lower unit (148–126 cm) to represent the wetland

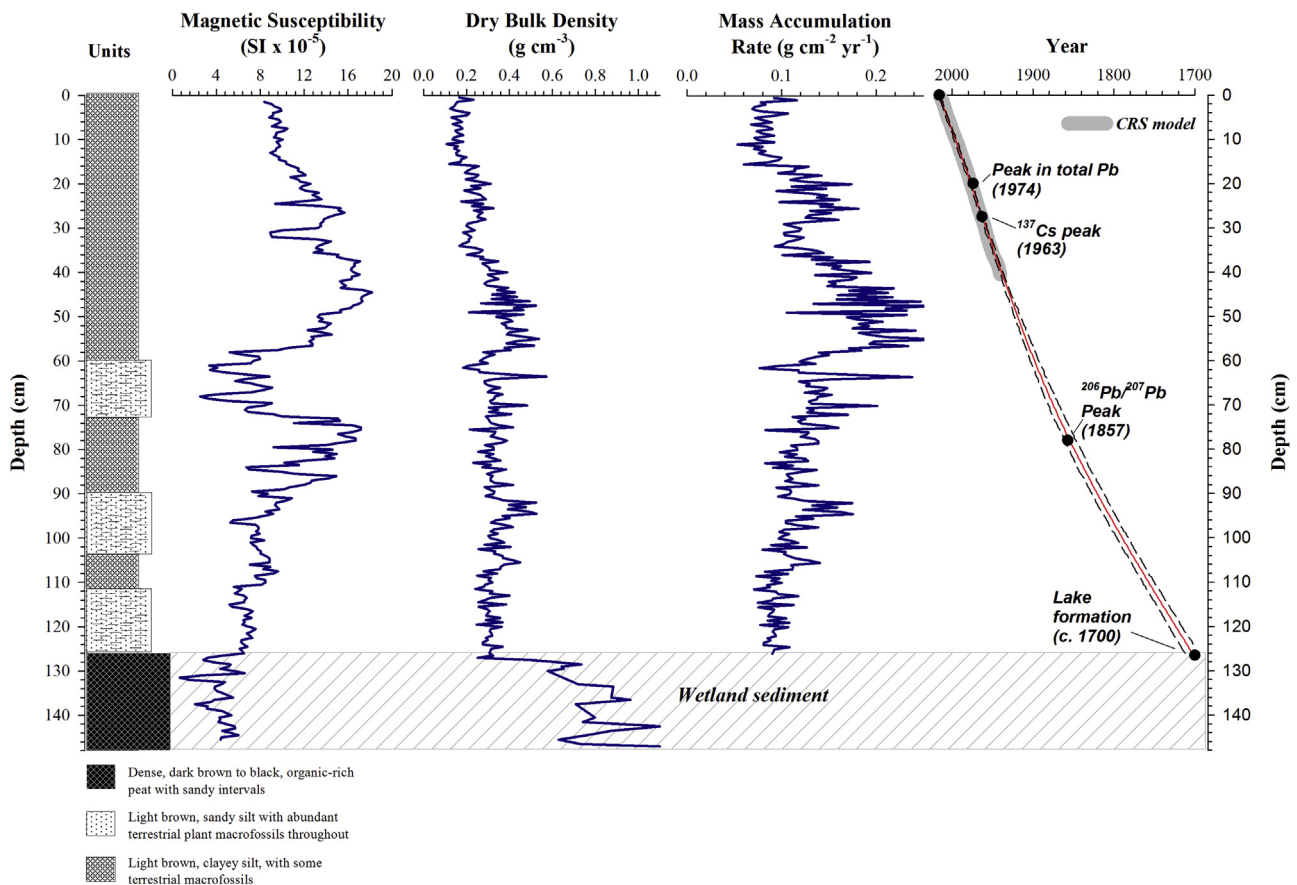


**Fig. 3.** Sedimentological data for core LMP-03-16 including magnetic susceptibility, dry bulk density and mass accumulation rate. An age-depth model (solid red line) was developed using several chronostratigraphic horizons with the Clam age modeling package (Blaauw, 2010). The 95% confidence limits of the Clam model are shown (dashed lines) and the age-depth information independently developed for the upper section of the core by applying a constant rate of supply model (CRS) to the excess  $^{210}\text{Pb}$  data. (For interpretation of the references to colour in this figure legend, the reader is referred to the web version of this article).

environment present in the valley before the construction of the dam that formed Lake Matoaka, and subsequent lacustrine deposition from 126–0 cm is where we focus our sedimentological and geochemical analyses.

#### 4.2. $^{210}\text{Pb}$ and $^{137}\text{Cs}$ activity

The  $^{210}\text{Pb}$  and  $^{137}\text{Cs}$  profiles show distinct changes with depth that were used to establish age control points (Fig. 4). The  $^{137}\text{Cs}$  profile shows no detectable ( $<0.1$  Bq/kg) activity below 41 cm, a sharp rise of  $^{137}\text{Cs}$  at 34.5–36.5 cm, and a prominent activity maxima (46 Bq/kg) at 27.5 cm followed by a decline in values to 10 cm where values then stabilize around 8 Bq/kg to the top of the core. Excess  $^{210}\text{Pb}$  activities have only minor fluctuations below 40.5 cm and are equivalent to  $^{226}\text{Ra}$  and thus assumed to be non-atmospheric beneath this depth (Fig. 4). We attribute the maximum  $^{137}\text{Cs}$  value at  $27.5 \pm 0.5$  cm to CE 1963, the peak in global fallout from nuclear weapons testing (Beck and Bennett, 2002). This age indicates a sedimentation rate of  $0.52 \pm 0.01$  cm/yr over the last 53 years (CE 2016–1963). We applied a constant rate of supply model (CRS) to excess  $^{210}\text{Pb}$  values (Appleby, 2001) which indicates that the upper 42 cm spans the last 80 years (CE 2016–1936). The  $^{137}\text{Cs}$  data independently confirms the  $^{210}\text{Pb}$  CRS ages and, taken together defines an average sedimentation rate of 0.52 cm/yr over the last c. 80 years.

#### 4.3. Total Pb concentrations

Total Pb concentrations range from 3.37 to 134  $\mu\text{g/g}$  (Fig. 4). Pb concentrations at the bottom of the lacustrine unit (126–94 cm) are relatively constant, averaging 11.4  $\mu\text{g/g}$ . We interpret this consistency as naturally occurring geogenic Pb. Above this interval, a small peak is evident at 23.2  $\mu\text{g/g}$  from 82–78 cm. Closer to the top, a pronounced peak is clear with maximum Pb concentrations of 134  $\mu\text{g/g}$  from 20.5–14.5 cm (Fig. 4). These trends are also observed in Pb data derived by scanning XRF, which provide a higher resolution perspective (Fig. 4). We also present the Pb concentration data relative to the percentage of silt and clay within each sample (%fines) (Fig. 4). Given that Pb is most often associated

with high surface area fine-grained particles, this normalizes atmospheric Pb concentrations relative to changes in the input of fine sediments (e.g. Aalto et al., 2003). Overall, similar features are evident throughout the record, but the deeper peak in values at 72–78 cm is more pronounced indicating a significant change in Pb input to the lake at that time. In addition to documenting Pb accumulation rates, we correlate the maximum values in Pb concentrations at 20.5–14.5 cm to the peak in Pb combustion in the U.S. This peak has been used by others as a chronostratigraphic marker to indicate a date of c. CE 1974 (e.g. Kemp et al., 2012). Assigning CE 1974 to this range of core depths indicates a sedimentation rate of  $0.42 \pm 0.07$  cm/yr, which is consistent with the rates of sedimentation we determined using radionuclides ( $\sim 0.5$  cm/yr) for the upper part of the core.

#### 4.4. Pb isotopes – $^{206}\text{Pb}/^{207}\text{Pb}$

The  $^{206}\text{Pb}/^{207}\text{Pb}$  values range from 1.18 to 1.22 (Fig. 4). Below 84 cm,  $^{206}\text{Pb}/^{207}\text{Pb}$  values show little variability and average 1.19. At 83 cm, the values sharply increase to a distinct peak of 1.22 at 78 cm, which correlates to an increase in Pb concentrations, most apparent when normalized to %fines. Above 83 cm, a gradual decline in values is evident up to 35 cm, and a general increasing trend above 35 cm. Trends in Pb isotopes suggest changes in pollution sources. Most significantly,  $^{206}\text{Pb}/^{207}\text{Pb}$  values show a contribution from the UMV in the 19<sup>th</sup> century, which has been found to have distinctly high  $^{206}\text{Pb}/^{207}\text{Pb}$  values of 1.3–1.5 (Heyl et al., 1959, 1974). We correlate the peak in values at 78 cm to c. AD 1857–1858 when the contribution of Pb from UMV was the highest, which has been documented at other sites in the eastern U.S. (Lima et al., 2005; Marcantonio et al., 2002; Kelly et al., 2009; Kemp et al., 2012).

#### 4.5. Chronology

The radionuclide data and several chronostratigraphic horizons provided the chronology for the record (Fig. 3). We interpret the lithologic transition that marks the onset of lacustrine sedimentation and initial formation of Lake Matoaka, c. CE 1700. Peaks in Pb

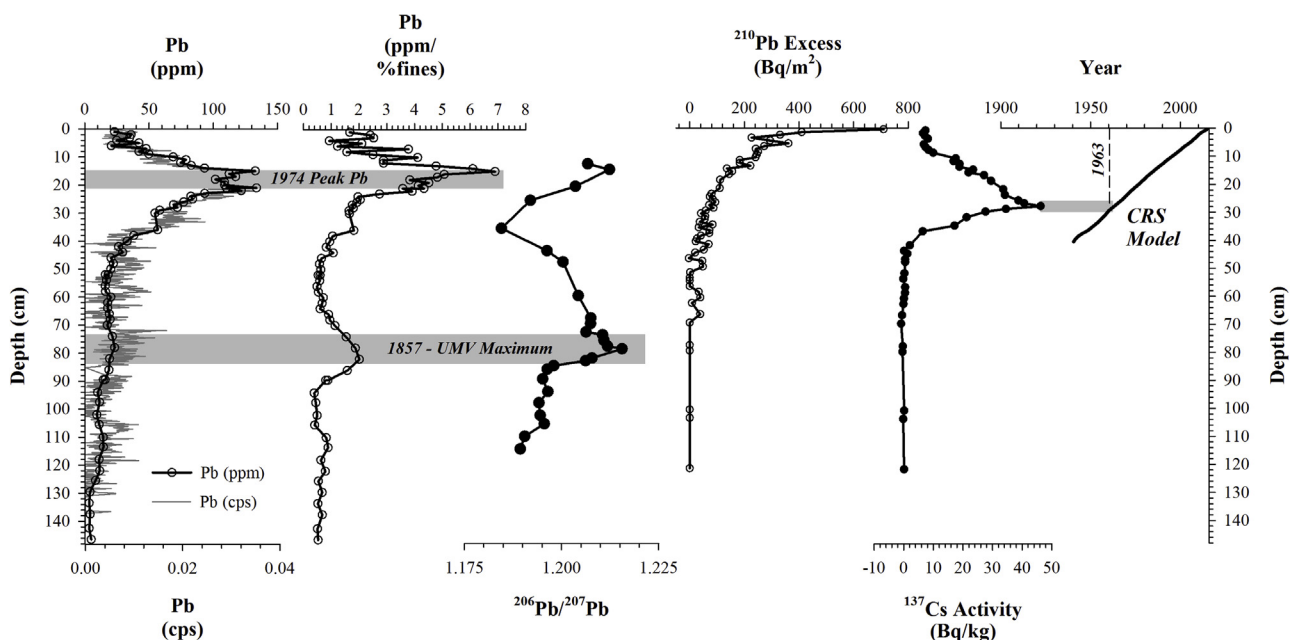


**Fig. 4.** Pb concentrations,  $^{206}\text{Pb}/^{207}\text{Pb}$ ,  $^{210}\text{Pb}$ , and  $^{137}\text{Cs}$  data for core LMP-03-16. Pb concentrations are presented from discrete measurements based nitric acid extractions (open circles), from scanning XRF analysis (gray line), and relative to the percentage of silt and clay (%fines).



concentrations and isotope values established age-control points correlated with maximum contributions of atmospheric Pb to Lake Matoaka sourced from UMV emissions c. AD 1857–1858, and the peak in U.S. Pb emissions in CE 1974. The peak in  $^{137}\text{Cs}$  correlated with the peak in atmospheric nuclear weapons testing fallout in CE 1963, and the date for the top of the core, CE 2016, is based on the year of collection.

An age-depth model was created using the Clam modeling package (Blaauw, 2010) in R (v. 3.0.1; R Development Core Team, 2011). A smooth-spline function was fitted to the ages, with model age uncertainties (2 sigma) from 2 to 19 years averaging 10 years. Uncertainties are significantly lower (3 years) in the upper 40 cm (CE 2016–1938) where more age control points were available. The  $^{210}\text{Pb}$ -based CRS model was not included, but independently confirms the age model and sedimentation rates from CE 2016–1938 (Fig. 3). The model shows an average sedimentation rate of 0.40 cm/yr for the entire record. Mass accumulation rates ( $\text{g}/\text{cm}^2/\text{yr}$ ) were determined using the age model and dry bulk density values (Fig. 3).

#### 4.6. Organic matter properties

Average TOC values are 6% with a range from 3 to 10% displaying several significant trends. There are several periods of higher values during the 18<sup>th</sup> and 19<sup>th</sup> centuries (c. CE 1700–1740, CE 1784–1795, CE 1871–1893), and values display an increasing trend that began c. CE 1920 and increased after c. CE 1980. The C/N values range from 9 to 20. Prior to CE 1910 values are higher and generally co-vary with TOC, however they deviate from this trend after c. CE 1910 (Fig. 6). Values for BSi range from 0.6 to 2.4%. Values are higher following the formation of the lake until c. CE 1820, and decrease from c. CE 1820 to c. CE 1910. After c. CE 1910, BSi values gradually increase to CE 2016 with an abrupt increase c. CE 2000. Values for sulfur are generally low with an average of 0.4%, but show a slight increasing trend after c. CE 1920 and a sharp increase after c. CE 1980.

Most significant are the systematic trends in the data before and after c. CE 1910 (Figs. 5 and 6). From c. CE 1700–1910, average C/N values are 14 and are strongly correlated with TOC ( $r^2 = 0.725$ ) indicating that terrestrial plants had a significant contribution to

sedimentary organic matter. The decline in BSi indicates a progressive decrease in surface water productivity, and low sulfur values with a high C/S (average = 20) suggest the presence of primarily organic-bound sulfur (Fig. 5). After c. CE 1910, the relationship between TOC and C/N changes with TOC more strongly correlated with BSi ( $r^2 = 0.6942$ ). This trend suggests that organic carbon was primarily from aquatic sources, and that the increasing trend in TOC and BSi resulted from an increase in surface water productivity from c. CE 1910–2016. The rapid rise in sulfur beginning c. CE 1980 and lower C/S suggest the source was inorganic sulfide under anoxic conditions.

#### 4.7. Grains size distributions

Grain size distributions throughout the record average 59% silt, 27% clay, and 14% sand. Significant variations exist across stratigraphic units and, in particular, before and after c. CE 1910 (Fig. 7). The sediment is generally coarser in composition and pulses of coarse sediment ( $>0.5\text{ mm}$ ) are evident from CE 1700–1910. After CE 1910, the composition of sand was lower and the amount of clay progressively increased to 42%. At c. CE 1975, another shift is evident to higher percentages of sand and lower percentage of clay, as well as more variability in the grain size data to CE 2016.

#### 4.8. Scanning XRF data

Statistical analysis of the XRF data revealed common trends and dominant modes of variability (Fig. 8). Correlation coefficients show that some of the elements are highly correlated ( $R > 0.70$ ) (Table 1). In particular, Si, K, and Ti, commonly sourced from siliclastics, are all highly correlated. The elements of Ca and Sr also show a high correlation, which likely reflects their common valence and association with fossils common in the Yorktown Formation (Mixon et al., 1989). The elements Mn and Zn show the highest correlation coefficient due to their similar biogeochemical behaviors ( $R = 0.87$ ) (Table 1). Results of PCA of the entire record (c. CE 1700–2016) shows the leading mode of variability (PC1) only accounts for 33% of the total variance (Figs. 7 and 8). Surprisingly, factor loadings reveal the highest correlations between PC1 and

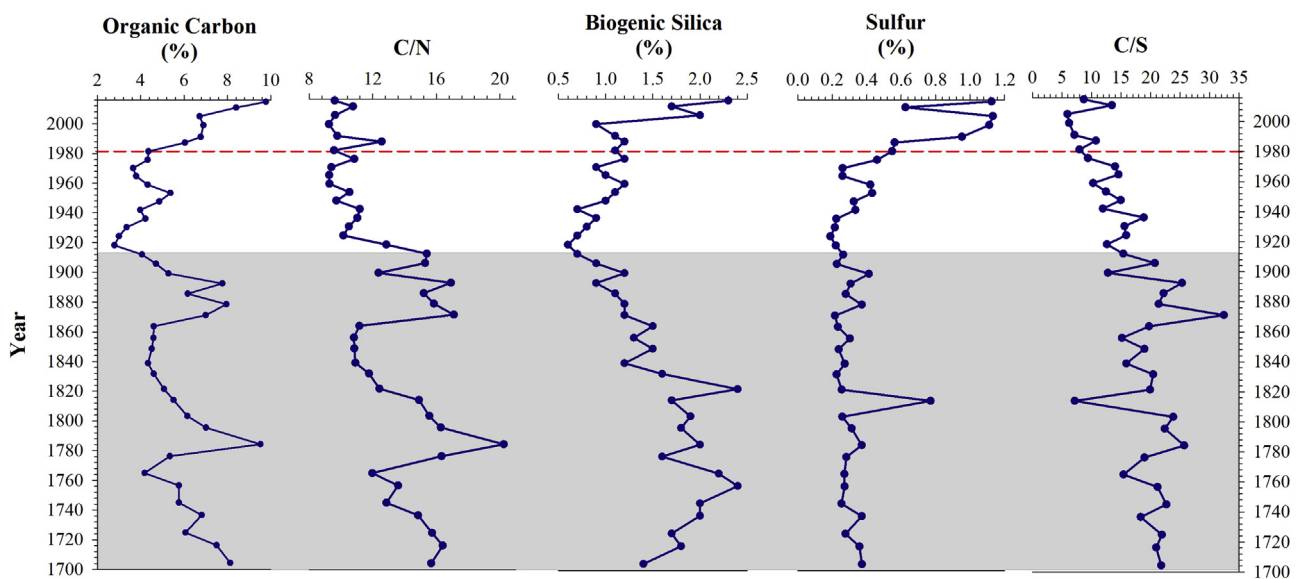


**Fig. 5.** Organic carbon, organic carbon to nitrogen ratios (C/N), biogenic silica, sulfur, and organic carbon to sulfur ratios (C/S) for core LMP-03-16. Gray shading distinguishes the earliest phase of sedimentation c. CE 1700–1910 from sedimentation after modification of the outlet c. CE 1910. Red dashed line defines changes c. CE 1980 when parameters indicate the onset of lake eutrophication. (For interpretation of the references to colour in this figure legend, the reader is referred to the web version of this article).

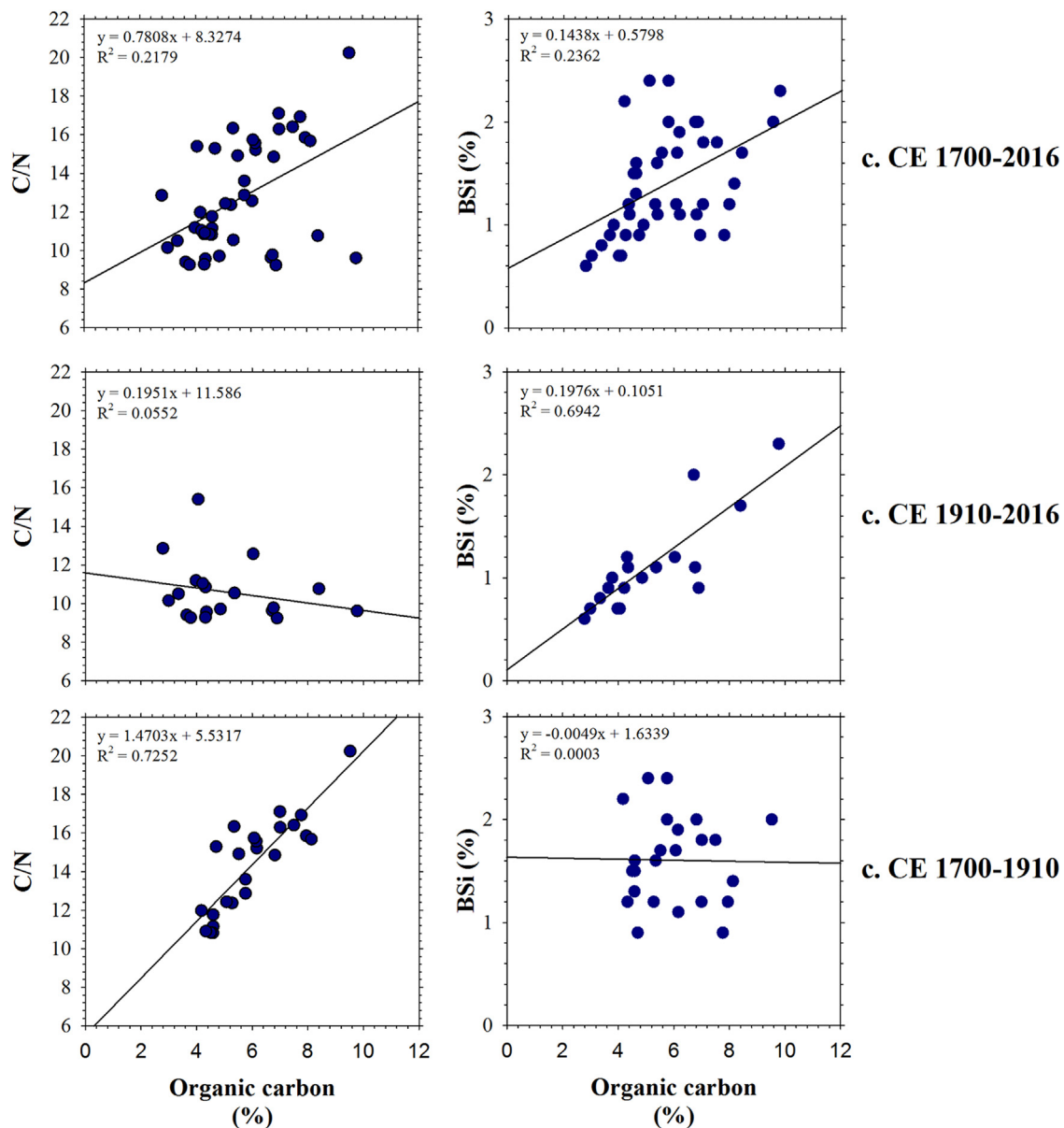


**Fig. 6.** Correlations between organic matter properties for the entire record (c. CE 1700–2016), and the intervals of sedimentation before and after modification of the outlet c. CE 1910 (AD 1700–1910 and CE 1910–2016).

element profiles of S, Mn, Zn, Zr, and Pb, and low correlations with lithogenic-derived elements: Si, K, and Ti. Trends in PC1 reveal a distinct change in variability c. CE 1910. Prior to CE 1910 variation are minor, but after CE 1910 there is a sharp change and an overall increase in values. The PCA performed on subsets of the elemental data from CE 1700–1910 and CE 1910–2016 reveal characteristics of sedimentation before and after this transition (Fig. 8). From c. CE 1700–2016, PC1 still accounts for only 34% of the variance. The PC1 is highly correlated with K and Fe and other lithogenic elements (Si, Ti), and inversely correlated with Ca. From c. CE 1910–2016, PC1 accounts for a higher percentage of the total variance (44%). The PC1 during this interval is highly correlated with elements associated with redox processes (S, Mn, Cu, Zn) and inversely correlated with lithogenic elements (Si, K, Ti). Overall, these data show a change in the influence of lithogenic input on sedimentation c. CE 1910, and the increase in the dominance of biological/redox processes on sedimentation after c. CE 1910.

## 5. Discussion

The sedimentological and geochemical data from Lake Matoaka define 2 distinct historical periods related to the development of the catchment and operation of the mill. The first period starts with the formation of the lake (c. CE 1700) and includes the lake's early history (c. CE 1700–1910) when it was used to operate a gristmill. The onset of the second period is marked by the stabilization of the lake (c. CE 1910), and spans the lake's recent history (c. CE 1910–2016), including the termination of mill operations and a progressive increase in development within the catchment.

### 5.1. Lake formation: c. CE 1700

The initial formation of Lake Matoaka is defined by an abrupt change from sandy peat to less dense sediment composed mostly



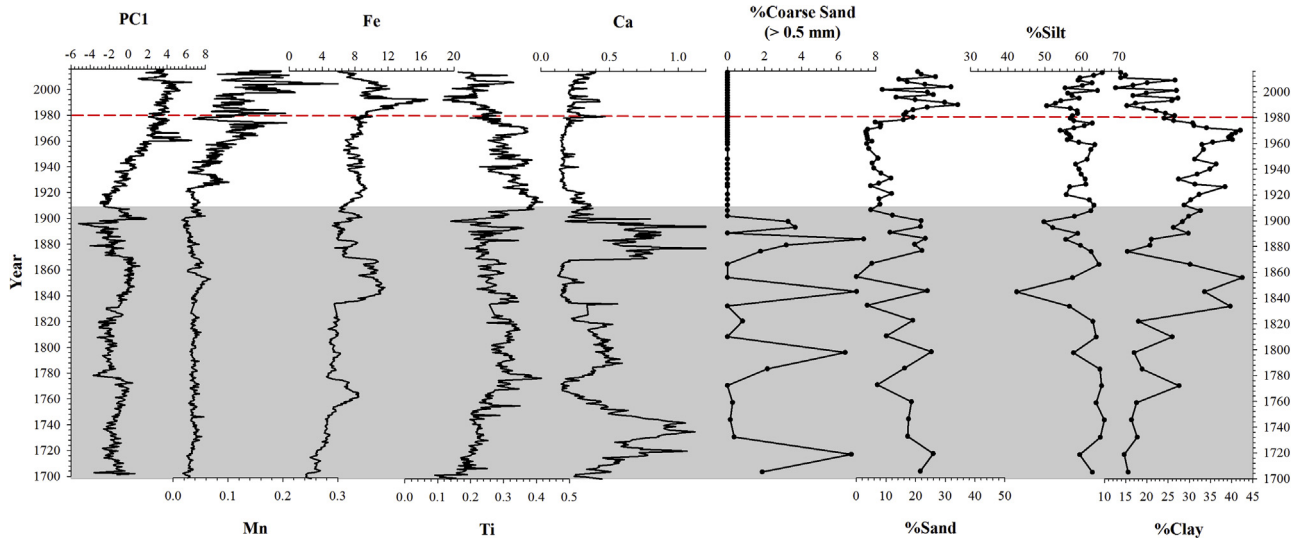


**Fig. 7.** Select scanning XRF elemental data, including the first principal component (PC1) of the entire dataset, and grains size analysis data from core LMP-03-16. Gray shading distinguishes the earliest phase of sedimentation c. CE 1700–1910 from sedimentation after modification of the outlet c. CE 1910. Red dashed line defines changes c. CE 1980 when parameters indicate the onset of lake eutrophication (For interpretation of the references to colour in this figure legend, the reader is referred to the web version of this article).

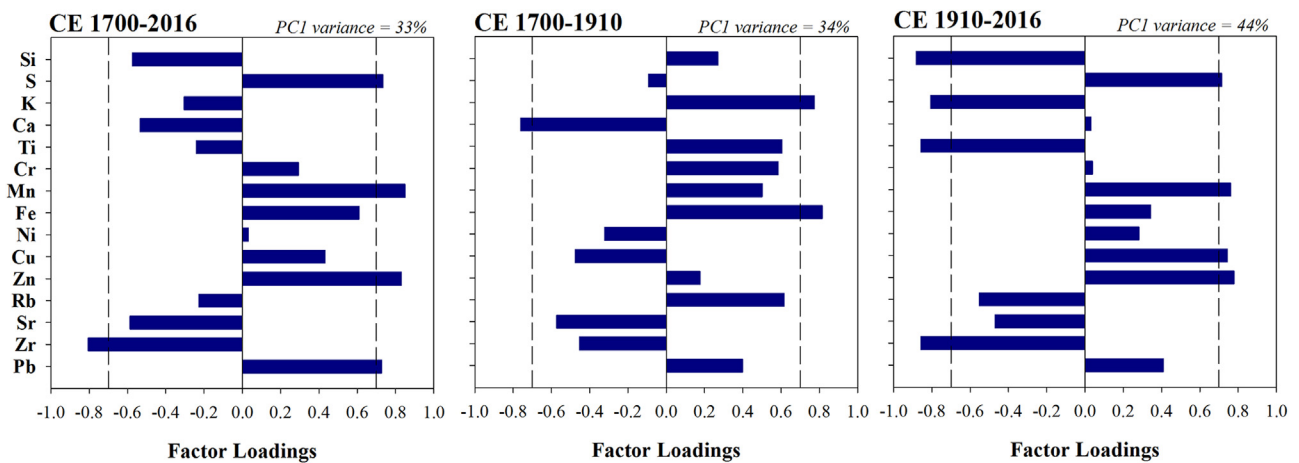


**Fig. 8.** Principal component analysis (PCA) results, including the variance of PC1 and factor loadings for PCA analyzed for the intervals c. CE 1700–2016, AD 1700–1910, and CE 1910–2016.

of silt and clay. The peat represents a wetland environment within the valley and the abrupt transition marks the onset of lacustrine deposition. Historic maps and property records indicate that the basin originally contained a wetland, Archer's Hope Swamp, with Archer's Hope Creek as the primary channel in the main valley, which today is named College Creek. At this time the area was referred to Middle Plantation, the first inland settlement of the Virginia colony (CE 1632–1699). Property records indicate that the lake was formed c. CE 1700 when a dam was constructed across Archer's Hope Creek to power a gristmill known as Ludwell's Mill and later Jones' Mill (Will of William Broadribb, 1905; Stephenson, 1947; Chappell, 1971). This was a period of agrarian expansion when many dams were constructed on the Coastal Plain of Virginia associated with mid-17<sup>th</sup> century acts passed to encourage their construction and to regulate the use of mill dams (Stephenson, 1947). The approximate date of lake formation also coincides with the establishment of Williamsburg in CE 1699 as the colonial capital of Virginia, which was followed by expansion of the town and increased commercial activity in the early 18<sup>th</sup> century (Morgan, 2004).

## 5.2. Impacts of early agricultural activities and mill operation: c. CE 1700–1910

From c. CE 1700–1990, sedimentation in Lake Matoaka was characterized by significant fluctuations in grain size, organic matter properties, and provenance. Grain size and XRF data show that sedimentation was controlled by lithogenic-derived elements, indicating primarily coarser clastic input (Fig. 7). Variations in TOC, which covary with C/N, reveal several periods of increased terrestrial-derived organic matter defined by broad increases in these parameters (c. CE 1720–1750, 1790–1840, and 1870–1900) (Figs. 5 and 6). These intervals are also marked by coarser sediment with high Ca and Sr values, attributed to silt and sand-sized shell fragments derived from the Miocene Yorktown Formation, a highly fossiliferous sedimentary layer that makes up the lake shoreline.

Historic data indicates that the catchment was mostly used for agriculture throughout this interval and likely had a greater impact on sedimentation than natural climate or environmental factors. Several possible mechanisms could explain these trends, including changes in catchment erosion, runoff, or lake-level. Sediment

delivery to the lake may have varied from land-use changes, deforestation, or other agricultural activity, which would have periodically destabilized parts of the catchment and increased erosion. Runoff may have fluctuated from reductions in stream flow from upstream water withdrawals or the emplacement of smaller dams on tributary streams. Today there is some evidence for at least two small former dams in the upper reaches of both Strawberry Creek and Pogonia creeks possibly used as ponds for cattle or irrigation, although the exact age of these features is unknown. Lake level fluctuations may have occurred from changes in runoff, mill operation, or the structural integrity of the dam, which may have been destroyed periodically from storms. Falling lake levels would have caused shoreline migration affecting the position of deltas relative to our coring location, increasing terrestrial organic matter inputs and coarser-grained sediment.

Williamsburg experienced population changes and several dramatic political and economic events, including several military conflicts from CE 1700–1900 (Morgan, 2004). By CE 1700, much of the lake's catchment was likely already used for agriculture. The 18<sup>th</sup> century (c. CE 1700–1775) was marked by increased construction of buildings, commercial, and government activity, as well as population growth, which reached approximately 1,500–2,000, but frequently supported more residents during large government assemblies (Morgan, 2004). This changed during the Revolutionary War (CE 1775–1783), when Williamsburg experienced considerable damage and was at one point occupied by the British Army. Interestingly, a map created during the war shows French and Continental Army encampments within the watershed of Lake Matoaka in CE 1782 (Fig. 1B; Desandroüins, 1782). However, in CE 1780 the capital of Virginia moved to Richmond, causing economic decline and stagnation that was compounded by national post-Revolutionary War depression. By CE 1783, half of the population had left, although it rebounded to ~1200–1500 by CE 1800 where it remained until c. CE 1850 (Morgan, 2004). Williamsburg was also at the center of conflicts during the Civil War (CE 1861–1865), which resulted in destruction of the town and postwar economic hardship. A historical map indicates that the dam impounding Lake Matoaka was destroyed during this interval (Gilmer, 1864) and a letter makes reference to the confederate army rebuilding the dam (Dubbs, 2002). The late 19<sup>th</sup> century was marked by renewed economic growth concurrent with national economic trends and locally associated with the construction of a railroad through Williamsburg and the surrounding region. This revival is reflected in the population of the town, which rose 80% between CE 1880–1910 to over 2700 (Morgan, 2004).

Based on this historical information, it is difficult to assign one specific mechanism or series of events to explain trends in sedimentation. However, it does show a significant number of intervals where the population and the economic stability of Williamsburg varied, which likely impacted mill operations and the overall agricultural activity of the surrounding land resulting in a high degree of variability in sedimentation. We did not observe any evidence for erosive events that could have resulted from modification/destruction of the dam, but we interpret what appear to be repeated abrupt changes in sediment composition from c. CE 1700–1910 to reflect the general instability of the dam and land use change described by historic maps and documents. These abrupt changes in sedimentary dynamics stop in c. CE 1910, which marks the onset of a period of greater stability in sedimentation.

### 5.3. Lake stabilization: c. CE 1910

Approximately c. CE 1910 marks an abrupt decrease in the average grain size, a shift to aquatic-sourced organic matter, and a change in the variability of elemental data represented by PC1. These data show a decrease in the amount and variability of

lithogenic and terrestrial input that indicates an overall higher and more stable lake level. The timing of this change corresponds roughly to when Jamestown Road was paved for the first time, the dam was widened, and when the operation of the gristmill stopped. Work to pave Jamestown Road began in December 1906 and was the first major project of the newly formed State Highway Commission for the State of Virginia (Virginia State Highway Commission, 1907). This project involved widening the dam in CE 1907 (Now grading near mill, 1907), and coincides with when mill operations ended around the start of World War I (Rouse, 1992). We interpret these changes to have more permanently controlled the outlet and stabilized the lake level to approximately its present elevation.

### 5.4. Impacts of 20<sup>th</sup> century development: c. CE 1910–2016

Following stabilization of the lake, there was a gradual increase in aquatic productivity evident by increasing TOC, along with decreasing Ti from catchment erosion. This interval is also marked by an increase in biologically relevant redox sensitive elements, which represent the majority of the variability as determined by PCA. Sedimentary Mn, Cu, S, and Zn generally increase in concentration during the 20<sup>th</sup> century, probably because they are necessary micronutrients for phytoplankton (Hecky and Kilham, 1988). These trends indicate a higher, more stable lake level and increased input of nutrients from greater development of the catchment.

The increase in nutrient input since c. CE 1910 reflects the growth of Williamsburg, including the massive reconstruction of the historic town center starting in the CE 1920s, and associated development of land within Lake Matoaka's watershed. We interpret finer-scale changes during this period as a result of better age control, and correlate some sedimentological and geochemical changes to specific historic events. From c. CE 1910–1945, mass accumulation rates are the highest of the entire record and likely reflect both the response of the catchment to stabilization of the dam, and increased development and deforestation in parts of the watershed (Fig. 9). Most notably, this period encompasses the early 20<sup>th</sup> century rapid population rise, and the development of an amphitheater associated with William & Mary on the lake's eastern shore. Another significant increase in mass accumulation rate (c. CE 1960–1980) can be correlated to increased runoff from construction of a large (c. 450,000 m<sup>2</sup>) paved commercial and residential area in the upper reaches of College Creek. Interestingly, mass accumulation rates have been relatively low since c. CE 1980, possibly in response to improved erosion control measures for modern construction projects and/or changes in sediment dynamics due to the installation of retention ponds to handle runoff from impervious surfaces. We also interpret the onset of eutrophication c. CE 1980 based on the rapid rise in TOC, BSi, and sulfur and low C/S ratios. This interval corresponds to a period when chronic sewage leaks into the lake resulted in excess nitrogen and phosphorus loading, leading to its current hyper-eutrophic designation (Nielson et al., 1990). Recent nutrient runoff has been curtailed, but internal loading of nitrogen and phosphorus continues to fuel algal blooms large enough to create “dead zones” of anoxic water during warm summer months.

### 5.5. History of local and regional atmospheric Pb deposition

The Lake Matoaka record provides a detailed perspective on historical atmospheric Pb pollution from local and regional industrial activity (Fig. 9). Local sources of Pb likely dominated accumulation from c. CE 1700 to 1775. During this period, there was a slow, systematic increase in Pb and a shift in Pb isotopes towards higher <sup>206</sup>Pb/<sup>207</sup>Pb values (Figs. 4 and 9). In the CE 1700s,

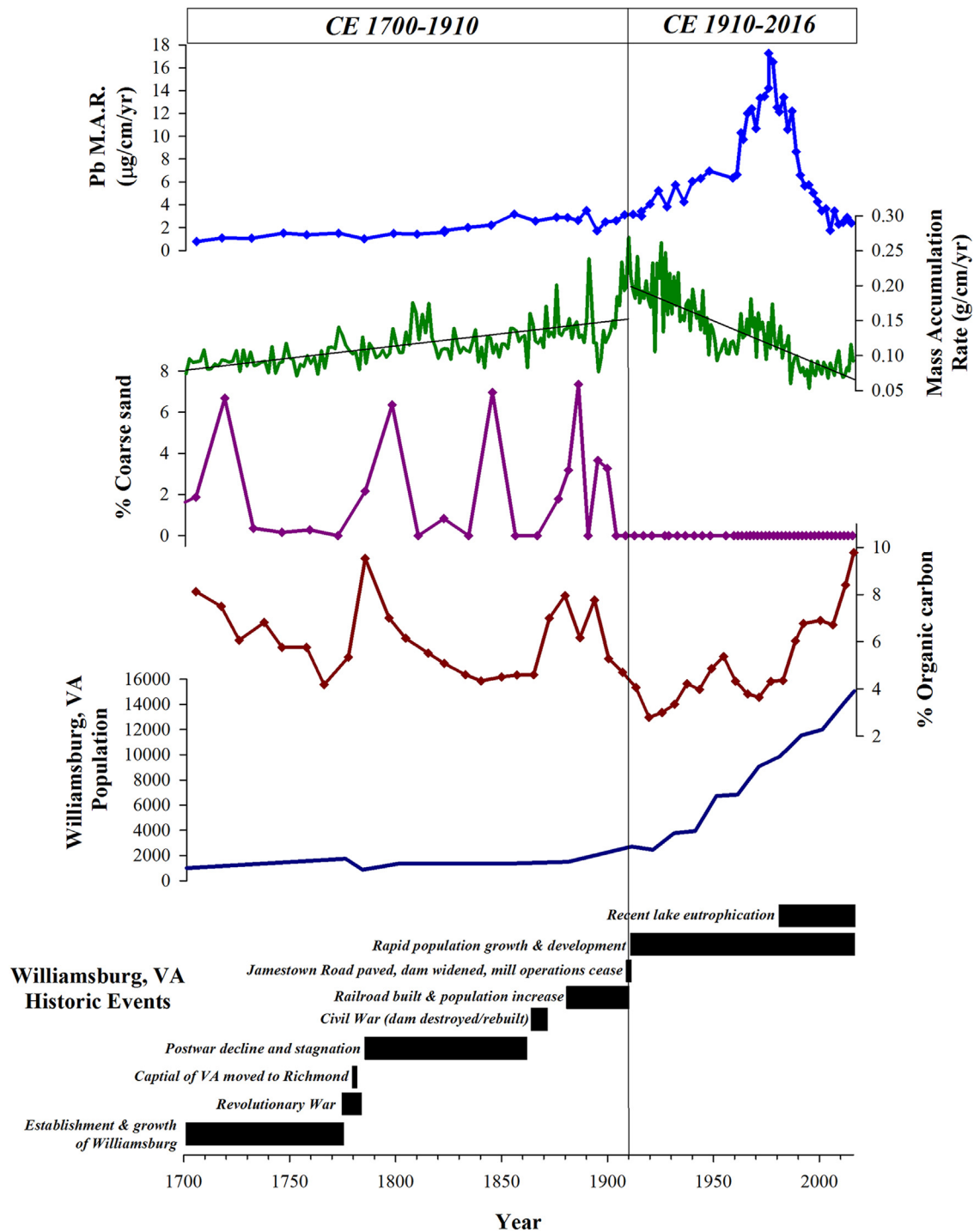


**Fig. 9.** Summary of select sediment parameters compared to the population of Williamsburg and important historic events since CE 1700 highlighting changes before and after CE 1910 (vertical line). Trend lines drawn for mass accumulation rates and were fitted to the data for the periods CE 1700–1910 and CE 1910–2016. Population data are estimates for specific time periods prior to CE 1900 as referred to by Morgan (2004) after which they are based on U.S. Census data.

the two major sources of Pb to the lake include geogenic Pb from weathered Tertiary coastal plain sediments and from coal combustion, which typically has higher  $^{206}\text{Pb}/^{207}\text{Pb}$  than primary silicate minerals (Chow and Earl, 1972). Coal extraction from the Richmond Basin, ~90 km west of Williamsburg, began in CE 1703 and was used locally for domestic fuel and in forges during the early to mid 18<sup>th</sup> century (Wilkes, 1988). Thus, early Pb accumulation data reflect local sources of pollution given that Williamsburg was a major center for economic, industrial, and military activity at that time. This trend stops c. CE 1780 with a

slight decrease in Pb accumulation, possibly attributed to the decline of industry in Williamsburg when the capital of Virginia moved to Richmond.

From the 19<sup>th</sup> to the early 21<sup>st</sup> century, Pb accumulation was dominated by more regional pollution sources. There is a steady increase from 1.5 to a broad maximum of  $3.5 \mu\text{g Pb}/\text{cm}^2/\text{yr}$  from c. CE 1800–1850, and the Pb isotopic composition shifted abruptly to the highest radiogenic Pb value of 1.216 (Fig. 4). As described above, these trends are consistent with the mining and smelting of Pb ores in the UMV (Lima et al., 2005; Kemp et al., 2012). This ore was



exhausted by c. CE 1870, and thus we (and others) see a decrease in Pb accumulation and a subsequent shift towards lower  $^{206}\text{Pb}/^{207}\text{Pb}$  from c. CE 1870–1900 (Fig. 9). During the early 20<sup>th</sup> century, Pb accumulation rose towards a local maximum (c.  $7 \mu\text{g Pb}/\text{cm}^2/\text{yr}$ ) in the CE 1940s reflecting an increase in the number of pollution sources. Interestingly, the isotopic composition drops to the lowest value measured ( $^{206}\text{Pb}/^{207}\text{Pb} = 1.18$ ), a trend that was also observed in Bermuda coral (Marcantonio et al., 2002). Sources of Pb to the environment at this time include Pb from coal combustion, smelting, and tetraethyl (TEL) Pb used as a gasoline additive (Graney et al., 1995). During the early 20<sup>th</sup> century, Pb ores used for gasoline were relatively low in  $^{206}\text{Pb}$  as U.S. Pb sources for TEL Pb shifted towards imports and geologically older Pb compared with Mississippi Valley ores (Hurst, 2000).

The most prominent feature of Pb accumulation is the maximum rate (c.  $17 \mu\text{g Pb}/\text{cm}^2/\text{yr}$ ) evident c. CE 1975, which is followed by a sharp decline (Fig. 9). This maxima has been identified in sediments from the Great Lakes (Graney et al., 1995), a remote pond in New Hampshire (Johnson et al., 1995), mid-Atlantic salt marshes (Kemp et al., 2012), tidal river basins (Lima et al., 2005), and offshore corals and marine sediments (Marcantonio et al., 2002). The  $^{206}\text{Pb}/^{207}\text{Pb}$  isotopic composition and high atmospheric deposition rate is attributed to peak use of TEL Pb, which dropped abruptly c. CE 1977 after Clean Air Act Amendments (Nriagu, 1990). Taken together, our Pb accumulation and isotopic data narrate a c. 300-year history of local and regional sources of Pb pollution in the mid-Atlantic U.S.

#### 5.6. Mill ponds as archives of regional landscape change

Sedimentation in mill ponds can vary based on the type of impoundment, which affects how they record past landscape changes or pollution history (Poff and Hart, 2002). Lake Matoaka is a low-gradient system impounded with a storage dam used to increase hydraulic head. Sedimentation is therefore dominated by finer-grained material, as compared to run-of-river dams, which create smaller hydraulic head and are higher energy systems (Csiki and Rhoads, 2010; Pearson and Pizzuto, 2015). Previous work has shown that impoundments similar to Lake Matoaka archive sediments and environmental contaminants, and profoundly affect local hydrology, geochemistry, sediment transport, and ecology (Evans et al., 2000; Smith et al., 2002; Arnason and Fletcher, 2003; Van Metre and Mahler, 2004; Mann et al., 2013; Fajer and Rzetala, 2018; Saulnier-Talbot and Lavoie, 2018).

Sediments archived in mill ponds can also be used to test sediment yield and landscape evolution models. In the eastern U.S., models have been developed to quantify the magnitude of landscape impacts on streams and watersheds following European settlement (Wolman, 1967; Jacobson and Coleman, 1986). Generally, these models show a gradual increase in sediment yields and floodplain aggradation from intense forest clearance and farming during the 18<sup>th</sup> and 19<sup>th</sup> centuries, followed by a decline to lower values in the early 1900's from farm abandoned, reforestation, and applications of soil conservation techniques. A sharp peak in sediment yields from construction, often an order of magnitude greater than previous intervals, marks the mid-20<sup>th</sup> century, followed by a gradual reduction in sediment supply as watersheds became urbanized (e.g. Wolman, 1967).

Mass accumulation rates in Lake Matoaka broadly reflect the trends described for other regions with similar land-use change histories allowing us to compare the application of these models to eastern Virginia (Wolman, 1967; Fig. 9). Lake Matoaka experienced a gradual increase in mass accumulation rates during the 18<sup>th</sup> and 19<sup>th</sup> centuries, rising from c.  $0.08\text{--}0.2 \text{ g}/\text{cm}^2/\text{yr}$ , likely from increased agricultural activity (Fig. 9). Similarly, the highest mass accumulation rates (c.  $0.28 \text{ g}/\text{cm}^2/\text{yr}$ ) occur during a period of construction in the mid-1900s, but generally decline thereafter. In

contrast to established sediment yield models, there was not an order-of-magnitude rise in sediment delivery from 20<sup>th</sup> century construction. Lake Matoaka seems to show a more muted response to significant changes in land use compared with predictions made from the Piedmont region of the mid-Atlantic U.S. (Wolman, 1967). Sediment storage in low-gradient stream channels may buffer sedimentation, which could be typical for coastal plain watersheds. Other studies have also shown that sediment storage and transport within a basin can be just as important as changes in land use, and can therefore affect the interpretation of past sediment yields (Evans et al., 2000).

## 6. Conclusions

This investigation of the sedimentary record from Lake Matoaka shows that the site has archived landscape changes and environmental impacts at high resolution since c. CE 1700. Results of multiple dating techniques show that sedimentation rates were high throughout the record,  $\sim 0.5 \text{ cm}/\text{yr}$ , which reflects both the nature of landscape changes within the catchment, as well as the influence of unconsolidated sedimentary units typical of the Atlantic Coastal Plain. We identify two important sedimentary intervals attributed to historic events in Williamsburg and the catchment of Lake Matoaka. The first period, from c. CE 1700–1910, includes when the lake was used to operate a gristmill and was susceptible to environmental impacts from early agricultural activities. The second period, c. CE 1910–2016, is characterized by a stabilization of sediment properties concurrent with the termination of mill operations, and a progressive increase in lake productivity, redox changes, and impacts of industrial contaminants. Our data provide a more comprehensive understanding of the evolution of Lake Matoaka and its catchment in the context of Williamsburg's history. We also document the history of Pb accumulation rates and demonstrate how they can be attributed to both local and regional pollution sources. More broadly, this study provides an example of how sediments accumulated in mill ponds or other artificial water bodies can provide clues to past anthropogenic environmental impacts and landscape changes. Our comparison to previously established sediment yield models for the region shows the importance of stream channel storage for Lake Matoaka, which may buffer pond sedimentation within similar low gradient, coastal plain landscapes.

## Acknowledgements

Funding was provided through a William & Mary (W&M) Faculty Research Grant to NLB, a W&M Department of Geology Ellen Stofan Scholarship to MGM, and a W&M Charles Center Research Award to MR. We would also like to thank Chuck Bailey for help designing mapped data, Briana Childs for assistance in the laboratory, and two anonymous reviewers for comments on an earlier draft.

## References

- Aalto, R., Maurice-Bourgoin, L., Dunne, T., Montgomery, D.R., Nitttrouer, C.A., Guyot, J.-L., 2003. Episodic sediment accumulation on Amazonian flood plains influenced by El Niño/Southern Oscillation. *Nature* 425, 493–497.
- Appleby, P.G., 2001. Chronostratigraphic techniques in recent sediments. In: Last, W.M., Smol, J.P. (Eds.), *Tracking Environmental Change Using Lake Sediments, Volume 1: Basin Analysis, Coring, and Chronological Techniques*. Kluwer Academic Publishers, Dordrecht.
- Arnason, J.G., Fletcher, B.A., 2003. A 40+ year record of Cd, Hg, Pb, and U deposition in sediments of Patroon Reservoir, Albany County, NY, USA. *Environ. Pollut.* 123, 383–391.
- Battarbee, R.W., Jones, V.J., Flower, R.J., Cameron, N.G., Bennion, H., Carvalho, L., Juggins, S., 2001. Diatoms. In: Smol, J.P., Birks, H.J.B., Last, W.M. (Eds.), *Tracking Environmental Change Using Lake Sediments, Vol. 3, Terrestrial, Algal, and Siliceous Indicators*. Kluwer Acad., Dordrecht, Netherlands, pp. 155–202.

- Beck, H.L., Bennett, B.G., 2002. Historical overview of atmospheric nuclear weapons testing and estimates of fallout in the continental United States. *Health Phys.* 82, 591–608.
- Blaauw, M., 2010. Methods and code for “classical” age-modelling of radiocarbon sequences. *Quat. Geochronol.* 5, 512518.
- Bollhofer, A., Rosman, K.J.R., 2000. Isotopic source signatures for atmospheric lead: the Southern Hemisphere. *Geochim. Cosmochim. Acta* 64, 3251–3262.
- Bollhofer, A., Rosman, K.J.R., 2001. Isotopic source signatures for atmospheric lead: the Northern Hemisphere. *Geochim. Cosmochim. Acta* 65, 1727–1740.
- Boyle, E.A., Chapnick, S.D., Shen, G.T., Bacon, M., 1986. Temporal variability of lead in the western North Atlantic. *J. Geophys. Res.* 91, 8573–8593.
- Caverly, E., Kaste, J.M., Hancock, G.S., Chambers, R.M., 2013. Dissolved and particulate organic carbon fluxes from an agricultural watershed during consecutive tropical storms. *Geophys. Res. Lett.* 40, 1–6.
- Chappell, 1971. Ludwell's Mill, Williamsburg, James City County. Archaeological Site Report (44WB0017). Virginia Department of Historic Resources, Richmond, Virginia.
- Chillrud, S.N., Hemming, S., Shuster, E.L., Simpson, H.J., Bopp, R.F., Ross, J.M., Pederson, D.C., Chaky, D.A., Tolley, L.-R., Estabrooks, F., 2003. Stable lead isotopes, contaminant metals and radionuclides in upper Hudson River sediment cores: implications for improved time stratigraphy and transport processes. *Chem. Geol.* 199, 53–70.
- Chow, T.J., Earl, J., 1972. Lead isotopes in North American coals. *Science* 176, 510–511.
- Conley, D.J., 1988. Biogenic silica as an estimate of siliceous microfossil abundance in Great Lakes sediments. *Biogeochemistry* 6, 161–179.
- Conley, D.J., Schelske, C.L., 2001. In: Smol, J.P., Birks, H.J.B., Last, W.M. (Eds.), *Biogenic Silica, in Tracking Environmental Change Using Lake Sediments, Vol. 3, Terrestrial, Algal, and Siliceous Indicators*. Kluwer Acad., Dordrecht, Netherlands, pp. 281–293.
- Coxon, T.M., Odhiambo, B.K., Giancarlo, L.C., 2016. The impact of urban expansion and agricultural legacies on trace metal accumulation in fluvial and lacustrine sediments of the lower Chesapeake Bay basin, USA. *Sci. Total Environ.* 568, 402–414.
- Croudace, I.W., Rindby, A., Rothwell, R.G., 2006. ITRAX: description and evaluation of a new multi-function X-ray core scanner. In: Rothwell, R.G. (Ed.), *New Techniques in Sediment Core Analysis*, 267. Geological Society, London, Special Publications, pp. 51–564.
- Csiki, S., Rhoads, B.L., 2010. Hydraulic and geomorphological effects of run-of-river dams. *Prog. Phys. Geogr.* 34, 755–780.
- Cutshall, N.H., Larsen, I.L., Olsen, C.R., 1983. Direct analysis of  $^{210}\text{Pb}$  in sediment samples: self-absorption corrections. *Nucl. Instrum. Methods* 206, 309–312.
- Davis, R.B., Anderson, D.S., Dixit, S.S., Appleby, P.G., Schauffler, M., 2006. Response of two New Hampshire (USA) lakes to human impacts in recent centuries. *J. Paleolimnol.* 35, 669–697.
- Desandrouins, J.N., 1782. Armée de Rochambeau, 1782. Carte des environs de Williamsburg en Virginie où les armées française et américaine ont campés en Septembre 1781 [Map] Retrieved from the Library of Congress. <https://www.loc.gov/item/gm71002174/>.
- Dubbs, C.K., 2002. *Defend This Old Town*. Louisiana State University Press, Baton Rouge.
- Evans, J.E., Gottgens, J.F., Gill, W.M., Mackey, S.D., 2000. Sediment yields controlled by intrabasinal storage and sediment conveyance over the interval 1842–1994: Chagrin River, northeast Ohio, U.S.A. *J. Soil Water Conserv.* 55, 264–270.
- Fajer, M., Rzetala, M.A., 2018. Mill pond sediments as the indicator of the environment of the drainage area (an example of Liswarta River, Odra basin, Poland). *Environ. Sci. Pollut. Res.* 25, 5832–5847.
- Gilmer, J.F., 1864. Vicinity of Richmond and Parts of the Peninsula [map]. 1:80,000. Virginia Historical Society, Richmond, VA.
- Graney, J.R., Halliday, A.N., Keeler, G.J., Nriagu, J.O., Robbins, J.A., Norton, S.A., 1995. Isotopic record of lead pollution in lake sediments from the northeastern United States. *Geochim. Cosmochim. Acta* 59, 1715–1728.
- Hecky, R.E., Kilham, P., 1988. Nutrient limitation of phytoplankton in freshwater and marine environments: a review of recent evidence on the effects of enrichment. *Limnol. Oceanogr.* 33, 796–822.
- Heyl, A.J., Agnew, A., Lyons, E., Behre, C.Jr., 1959. The Geology of the Upper Mississippi Valley Zinc-lead District. Professional Paper 309. U.S. Geological Survey.
- Heyl, A.V., Landis, G.P., Zartman, R.E., 1974. Isotopic evidence for the origin of Mississippi Valley-type mineral deposits: a review. *Econ. Geol.* 69, 992–1006.
- Holmer, M., Storkholm, P., 2001. Sulphate reduction and sulphur cycling in lake sediments: a review. *Freshw. Biol.* 46, 431–451.
- Hurst, R.W., 2000. Applications of anthropogenic lead archaeostratigraphy (ALAS model) to hydrocarbon remediation. *Environ. Forensics* 1, 11–23.
- Jacobson, R.B., Coleman, D.J., 1986. Stratigraphy and recent evolution of Maryland piedmont flood plains. *Am. J. Sci.* 286, 617–637.
- James, L.A., 2013. Legacy sediment: definitions and processes of episodically produced anthropogenic sediment. *Anthropocene* 2, 16–26.
- Johnson, C.E., Siccama, T.G., Driscoll, C.T., Likens, G.E., Moeller, R.E., 1995. Changes in lead biogeochemistry in response to decreasing atmospheric inputs. *Ecol. Appl.* 5, 813–822.
- Kaste, J.M., Bostick, B.C., Friedland, A.J., Schroth, A.W., Siccama, T.G., 2006. Fate and speciation of gasoline-derived lead in organic horizons of the Northeastern USA. *Soil Sci. Soc. Am. J.* 70, 1688–1698.
- Kelly, A.E., Reuer, M.K., Goodkin, N.F., Boyle, E.A., 2009. Lead concentrations and isotopes in corals and water near Bermuda, 1780–2000. *Earth Planet. Sci. Lett.* 283, 93–100.
- Kemp, A.C., Sommerfield, C.K., Vane, C.H., Horton, B.P., Chenery, S., Anisfeld, S., Nikitina, D., 2012. Use of lead isotopes for developing chronologies in recent salt-marsh sediments. *Quat. Geochronol.* 12, 40–49.
- Kennedy, L., 2016. Nineteenth century legacy mill pond sediment in the Southern Blue Ridge. *Southeast. Geogr.* 56, 101–117.
- Lecce, S.A., Pease, P.P., Gares, P.A., Wang, J., 2006. Seasonal controls on sediment delivery in a small coastal plain watershed, North Carolina, USA. *Geomorphology* 73, 246–260.
- Lima, A.L., Bergquist, B.A., Boyle, E.A., Reuer, M.K., Dudas, F.O., Reddy, C.M., Eglington, E.I., 2005. High-resolution historical records from Pettaquamscutt River basin sediments: 2. Pb isotopes reveal a potential new stratigraphic marker. *Geochim. Cosmochim. Acta* 69, 1813–1824.
- Liu, E., Shen, J., Birch, G.F., Yang, X., Wu, Y., Xue, B., 2012. Human-induced changes in sedimentary trace metals and phosphorus in Chaohu Lake, China, over the past half-millennium. *J. Paleolimnol.* 47, 677–691.
- Mann, K.C., Peck, J.A., Peck, M.C., 2013. Assessing dam pool sediment for understanding past, present, and future watershed dynamics: an example from the Cuyahoga River, Ohio. *Anthropocene* 2, 76–88.
- Marcantonio, F., Zimmerman, A., Xu, Y., Canuel, E., 2002. A Pb isotope record of mid-Atlantic US atmospheric Pb emissions in Chesapeake Bay sediments. *Mar. Chem.* 77, 123–132.
- Markewich, H.W., Pavich, M.J., Buell, G.R., 1990. Contrasting soils and landscapes of the Piedmont and coastal plain, eastern United States. *Geomorphology* 3, 417–447.
- McConnell, J.R., Wilson, A.I., Stohl, A., Arienzo, M.M., Chellman, N.J., Eckhardt, S., Thompson, E.M., Pollard, A.M., Steffensen, J.P., 2018. Lead pollution recorded in Greenland ice indicates European emissions tracked plagues, wars, and imperial expansion during antiquity. *Proc. Natl. Acad. Sci.* 22, 5726–5731.
- Meyers, P.A., 2003. Applications of organic geochemistry to paleolimnological reconstructions: a summary of examples from the Laurentian Great Lakes. *Org. Geochem.* 34, 261–289.
- Mitchell, M.J., Schindler, S.C., Owen, J.S., Norton, S.A., 1988. Comparison of sulfur concentrations within lake sediment profiles. *Hydrobiologia* 157, 219–229.
- Mixon, R.B., Berquist, C.R., Newell, W.L., Johnson, G.H., Powars, D.S., Schindler, J.S., Rader, E.K., 1989. *Geologic Map and Generalized Cross Sections of the Coastal Plain and Adjacent Parts of the U.S. Geological Survey, Miscellaneous Investigations Series Map I-2033*, Piedmont, Virginia.
- Morgan, T.E., 2004. *Williamsburg: a City That Made History*. Arcadia Publishing, San Francisco CA, pp. 160.
- Mortlock, R.A., Froelich, P.N., 1989. A simple method for the rapid determination of biogenic opal in pelagic marine sediments. *Deep-Sea Res.* 36, 1415–1426.
- Murozumi, M., Chow, T.J., Patterson, C., 1969. Chemical concentrations of pollutant lead aerosols, terrestrial dusts, and sea salts in Greenland and Antarctica snow strata. *Geochim. Cosmochim. Acta* 33, 1247–1294.
- Nielson, B., Anderson, G.F., Rhodes, M., 1990. Eutrophication of Lake Matoaka Assessment and Projection. Virginia Institute of Marine Sciences Special Scientific Report No. 123.
- Niemitz, J., Haynes, C., Lasher, G., 2013. Legacy sediments and historic land use: chemostratigraphic evidence for excess nutrient and heavy metal sources and remobilization. *Geology* 41, 47–50.
- Now grading near mill, 1907. *Virginia Gazette* February 16. *Chronicling America: Historic American Newspapers*. Library of Congress, Williamsburg, VA. <http://chroniclingamerica.loc.gov>.
- Nriagu, J.O., 1979. Global inventory of natural and anthropogenic emissions of trace metals to the atmosphere. *Nature* 279, 409–411.
- Nriagu, J.O., 1990. The rise and fall of leaded gasoline. *Sci. Total Environ.* 92, 13–28.
- Pearson, A.J., Pizzuto, J., 2015. Bedload transport over run-of-river dams, Delaware, U.S.A. *Geomorphology* 248, 382–395.
- Pensa, M.A., Chambers, R.M., 2004. Trophic transition in a lake on the Virginia coastal plain. *J. Environ. Qual.* 33, 576–580.
- Pizzuto, J., O'Neal, M., 2009. Increased mid-twentieth century riverbank erosion rates related to the demise of mill dams, South River, Virginia. *Geology* 37, 19–22.
- Poff, N.L., Hart, D.D., 2002. How dams vary and why it matters for the emerging science of dam removal? *BioScience* 52, 659–668.
- Price, K., Leigh, D.S., 2006. Stream morphological and sedimentological response to human impact in the southern Blue Ridge Mountains USA. *Geomorphology* 78, 142–160.
- R Development Core Team, 2011. *R: A Language and Environment for Statistical Computing*. R Foundation for Statistical Computing, Vienna, Austria. [www.R-project.org](http://www.R-project.org).
- Ritchie, J.C., McHenry, R.J., 1990. Application of radioactive fallout Cesium-137 for measuring soil erosion and sediment accumulation rates and patterns: a review. *J. Environ. Qual.* 19, 215–233.
- Rosman, K.J.R., Chisholm, W., Hong, S., Candelone, J.P., Boutron, C.F., 1997. Lead from Carthaginian and Roman Spanish mines isotopically identified in Greenland ice dated from 600 BC to 300 AD. *Environ. Sci. Technol.* 31, 3413–3416.
- Rothwell, R.G., Hoogakker, B., Thomson, J., Croudace, I.W., Frenz, M., 2006. Turbidite emplacement on the southern Balearic abyssal Plain (western Mediterranean Sea) during Marine isotope stages 1–3: an application of ITRAX XRF scanning of sediment cores to lithostratigraphic analysis. In: Rothwell, R.G. (Ed.), *New Techniques in Sediment Core Analysis*. Special Publications, Geological Society, London, pp. 79–98.
- Rouse, P., 1992. *Mills Once Dotted Williamsburg Area*. August 16. Daily Press, Newport News, VA.

- Saulnier-Talbot, É., Lavoie, I., 2018. Uncharted waters: the rise of human-made aquatic environments in the age of the “Anthropocene.”. *Anthropocene* 23, 29–42.
- Smith, S.V., Rensick, W.H., Bartley, J.D., Buddemeier, R.W., 2002. Distribution and significance of small, artificial water bodies across the United States landscape. *Sci. Total Environ.* 299, 21–36.
- Stephenson, M.A., 1947. Mills in Eighteenth Century Virginia with Special Study of Mills Near Williamsburg. Colonial Williamsburg Foundation Library Research Report Series 116, Williamsburg, Virginia.
- Sturges, W.T., Barrie, L.A., 1987. Lead 206/207 isotope ratios in the atmosphere of North America as tracers of US and Canadian emissions. *Nature* 329, 144–146.
- Van Metre, P.C., Mahler, B.J., 2004. Contaminant trends in reservoir sediment cores as records of influent stream quality. *Environ. Sci. Technol.* 38, 2978–2986.
- Virginia State Highway Commission, 1907. First Annual Report of the State Highway Commissioner to the Governor of Virginia for the Year Ending September 30, 1907. Richmond, Virginia. , pp. 74.
- Walter, R., Merritts, D., 2008. Natural Streams and the legacy of water-powered mills. *Science* 319, 299–304.
- Wilkes, G.P., 1988. Mining history of the Richmond coalfields of Virginia. Virginia Div. Mineral Resour. Publ. 85, 51.
- Will of William Broadribb, 1905. Will of William Broadribb of James City County, Va. [sic] (May 3, 1703). *William Mary Q.* 14, 35–37.
- Wolman, M.G., 1967. A cycle of sedimentation and erosion in urban river channels. *Geogr. Ann. Ser. A Phys. Geogr.* 49, 385–396.